Available online at www.sciencedirect.com
ScienceDirect
Journal of Power Sources 167 (2007) 228–233
JOURNAL OF POWER SOURCES
www.elsevier.com/locate/jpowsour

Short Communication

Influence of rare earth content on Mm-based AB_5 metal hydride alloys for Ni-MH batteries—An X-ray fluorescence study

M.V. Ananth [a,*], M. Raju [a], K. Manimaran [a], G. Balachandran [b], Lekshmi M. Nair [c]

[a] *Ni-MH Section, Electrochemical Energy Sources Division, Central Electrochemical Research Institute, Karaikudi–630 006, India*
[b] *Special Melting Group, Defence Metallurgical Research Laboratory, Hyderabad–500058, India*
[c] *Department of Physics, Lady Doak College, Madurai–625002, India*

Received 24 November 2006; received in revised form 28 December 2006; accepted 2 January 2007
Available online 12 February 2007

Abstract

AB_5-type MH alloys with Mm (Misch metal) as the A part (with varied rare earth contents in Mm) were investigated for rare earth by XRF analysis and battery performance by life cycle tests with an objective of understanding the influence of rare earth content on electrochemical hydrogen storage. The La/Ce ratio was found to vary from 0.51 to 18.73. The capacity output varied between 179 and 266 mAh g^{-1}. The results show that the La/Ce ratio has a strong influence on the performance, with the best performance realized with samples having an La/Ce ratio of around 12. La enhancement facilitates easy activation due to refinement in grain size and interstitial dimensions. Also, an orderly influence on crystalline structure could be seen. The study demonstrates that the rare earth content is an essential factor in determining the maximum capacity output because of its influence on crystal orientation as well as an increase in the radius of the interstitials, lattice constants and cell volumes.
© 2007 Elsevier B.V. All rights reserved.

Keywords: Hydrogen storage alloys; Ni/MH batteries; X-ray fluorescence; La/Ce ratio; Crystalline structure

1. Introduction

Hydrogen storage alloys have been in the highlighted recently due to the projected importance of "Hydrogen Energy" [1]. An important aspect in the development of hydrogen as an energy carrier concerns the use of metal hydrides for hydrogen storage [2]. Metal hydrides such as those based on AB_5–type alloys are also amenable for chemical, mechanical or thermodynamic work as in electrochemical cells [3], hydrogen compressors [4,5] thermodynamic machines [6,7] and space projects [8]. Recently, the alloy $(La_{0.68}Ce_{0.17}Pr_{0.05}Nd_{0.10})Ni_{3.55}Co_{0.75}Mn_{0.40}Al_{0.30}$ was used in the production of sorbitol by electrolysis of glucose [9]. Rare earth-based AB_5-type alloys and Zr-based laves phase alloys have been exploited as negative electrode materials in commercial Ni/MH cells [10,11]. The AB_5-type hydrogen storage alloys have seen large-scale production in several countries, particularly Japan, USA and China [12,13]. Ni-MH batteries are seen as promising high-capacity portable power sources especially for electrical traction [14]. Investigations of AB_5-type rare earth-based hydrogen storage alloys are being pursued in order to improve their electrochemical characteristics and to reduce cost of production [15,16]. The discharge capacity of advanced AB_5-type negatives of Ni-MH batteries has reached 310–330 mAh g^{-1} [17]. Further improvement in the capacity of AB_5-type alloys seems to be difficult since the theoretical capacity of $LaNi_5$ is about 372 mAh g^{-1}. Moreover, low capacity of AB_5-type alloy electrodes and difficult activation characteristics of Laves phase alloy electrodes limit their extensive application [18,19]. The poor cycle stability of alloy electrodes is attributed to large expansion in cell volume as well as corrosion of La during the charge/discharge processes [20]. In recent years, however, Ni-MH cells face an additional threat in the form of competition from the burgeoning lithium-ion market [21]. Therefore, investigations into alloys with higher capacities and longer cycle life are crucial. However, the effect of rare earth content on electrode performance has received only scant attention [22,20].

Zhang et al. [22], who studied the effect of substituting Mm with La on the electrochemical performances of as-cast and quenched alloys, found that the substitution led to a marginal

* Corresponding author. Tel.: +91 4565 227553; fax: +91 4565 227713.
E-mail address: mvananth@rediffmail.com (M.V. Ananth).

0378-7753/$ – see front matter © 2007 Elsevier B.V. All rights reserved.
doi:10.1016/j.jpowsour.2007.01.091

increase in capacity retention and had an insignificant effect on the activation capabilities. The effect of La/Mg ratio on the structure and electrochemical properties of $La_xMg_{3-x}Ni_9$ ($x = 1.6$–2.2) ternary alloys was also investigated [20]. An increase in the La/Mg ratio led to increased cell volume and hydride stability.

Because La is costly, its replacement with the relatively cheaper Misch metal can be attractive. Permutations and combinations within permissible limits in the composition of Misch metal can vastly alter its properties. Among factors that can affect its properties, La/Ce ratio is believed to have a significant effect on electrochemical hydrogen storage. However, no detailed study is available in literature. Hence, in the present study, two series of AB_5 MH alloys (with low and high Mn contents) with Mm (with wide variations in rare earth content) in the A part have been investigated. While X-ray fluorescence was used for analyzing the rare earth content, charge–discharge cycling was used for assessing battery performance.

2. Experimental

AB_5 alloys of the type $MmNi_{3.5}Co_{0.8}Mn_{0.4}Al_{0.3}$ with extensive modifications in the A part (produced by arc melting at DMRL in collaboration with CECRI) were used for this study. The purity of the constituent elements was above 99 wt.%. Two series of alloys (with low and high Mn contents) were prepared. The alloys were annealed and crushed into powder (<75 μm). The test alloy (1 g) was mixed with KS44 graphite powder (20%), carbonyl nickel (10%) and silver oxide (10%). PTFE was used as binder and the active material paste was applied over a nickel foam substrate. The metal hydride electrode was compacted at an appropriate pressure and heated at 120 °C for 1 h. The geometric area of the negative electrode was 1 cm^2 and the thickness was 1.5 mm. For cycling studies, the negative electrode was sandwiched in between two sintered $NiOOH/Ni(OH)_2$ positive electrodes with a 'Scimat' separator. A 6 M solution of KOH was used as the electrolyte. A Bitrode LCN life cycle tester was employed for life cycle studies. Cells were tested at a C_5 rate to a discharge cut-off voltage of 1 V at 303 ± 1 K. In every cycle, the cells were overcharged by about 30% after a 15 min pause. XRF measurements were performed on a HORIBA XRF Analyzer in non-standard mode. XRD patterns were recorded on a PANalytical X'per PRO model diffractometer with Cu Kα (2.2 kW maximum) radiation. The XRD data were analyzed by a 'Crysfire' indexing package.

3. Results and discussion

3.1. Physical characterization

3.1.1. XRF analysis

The results of the XRF analysis are presented in Table 1. An objective in modifying $LaNi_5$-based hydrogen storage alloys with small amounts of La and Ni is to increase the cycling life of metal hydride electrodes. However, this modification sometimes causes an undesirable increase in the activation time and a decrease in the hydrogen storage capacity. Beneficial effects of substitution of La by Ce, Y, and Nd on the cycle life of metal hydride alloys have been reported [23–25]. In commercial AB_5-type metal hydride electrodes, quite good performance was obtained using Mm in place of La, where Mm is a naturally occurring mixture of the rare earth metals with a composition of (at.%) Ce: 50–55, La: 18–28, Nd: 12–18, and Pr: 4–6 [23]. Since Ce is the predominant rare earth metal in normal Mm, the role of this element has been investigated in more detail [25]. Results indicated an improvement in the cycle life due to the presence of Ce, and this effect has been attributed to the formation of a passivating layer of oxide on the alloy particle surfaces. It is well known that in such materials the La/Ce ratio is crucial in deciding the battery performance. The La/Ce ratios in the alloys are given in Table 2.

3.1.2. XRD analysis

The results of XRD analysis of selected MH alloys with low Mn content are shown in Fig. 1. It can be seen that the sample with an La/Ce ratio around 0.5 can assume a monoclinic crystalline structure whereas the samples with high La/Ce ratios assume a orthorhombic structure. A close examination of the XRD patterns also reveal that samples with very low La/Ce ratios had additional phases, while those with very high La contents had an additional hexagonal phase. The unit cell volume increases from 494.21 $Å^3$, corresponding to La/Ce ratios of around 0.5, reaching a maximum of 1161.83 $Å^3$ for samples with an La/Ce ratio of around 1, and stabilizes at around 796.25 $Å^3$ for samples with higher values. Some amorphous nature devel-

Table 1
XRF data of MH alloys

ALLOY	Al	Si	Mn	Fe	Co	Ni	La	Ce	Pr	Nd	Pm
Alloys with low Mn content (%)											
I	1.44	9.43	0.09	1.18	9.80	39.91	10.48	20.66	4.14	2.22	0.66
II	3.07	5.22	0.08	0.83	8.91	39.16	17.32	17.47	2.62	4.54	0.78
III	2.25	5.62	0.10	0.25	5.85	40.42	36.34	3.83	3.61	1.71	0.01
IV	1.48	6.29	0.00	0.16	7.50	37.80	41.79	3.33	0.40	1.23	0.02
V	1.63	5.53	0.06	0.13	8.30	38.11	39.70	2.12	3.01	1.40	0.00
Alloys with high Mn content (%)											
VI	0.81	6.40	5.04	0.22	8.98	36.90	11.02	21.25	6.19	3.18	0.02
VII	1.27	5.72	4.71	0.41	9.40	37.75	13.28	20.63	4.16	2.01	0.66
VIII	0.52	5.63	4.04	0.51	8.34	37.71	36.57	3.14	2.47	1.06	0.01

Table 2
Influence of rare earth content (La/Ce) on performance of MH alloys

Alloy	La Content	Ce Content	(La/Ce) Ratio	Max. capacity mAh g^{-1}
Alloys with low Mn content (%)				
I	10.48	20.66	0.51	186.00
II	17.32	17.47	0.99	210.00
III	36.34	3.83	9.49	223.00
IV	41.79	3.33	12.55	233.00
V	39.70	2.12	18.73	180.00
Alloys with high Mn content (%)				
VI	11.02	21.25	0.52	179.00
VII	13.28	20.63	0.64	188.00
VIII	36.57	3.14	11.65	266.00

ops for samples with La/Ce ratios around 1. There is a marked change in the values of the lattice parameters *a*, *b* and *c* for samples with La/Ce ratios up to around 10 (as seen in insets in Fig. 1). However, above this range the values of the lattice parameters get stabilized. Thus, an orderly influence of the La/Ce ratio on the XRD patterns can be seen in alloys with low Mn contents.

Results of the XRD analysis of selected MH alloys with high Mn contents are shown in Fig. 2. An La/Ce ratio of about 0.5 corresponds to a tetragonal crystal structure with a unit cell volume of 722.86 $\mathring{A}^3$. An La/Ce ratio of about 12 corresponds to an orthorhombic crystal structure with a unit cell volume of 528.73 $\mathring{A}^3$. It is seen that the unit cell volume decreases as the Mn content increases.

3.2. Electrochemical performances of the alloys

3.2.1. Discharge capacity and cycle life

The variation in the discharge capacity of the alloys as a function of cycle number is illustrated in Fig. 3(a and b). It is well known that fade in capacity for alloy electrodes can be

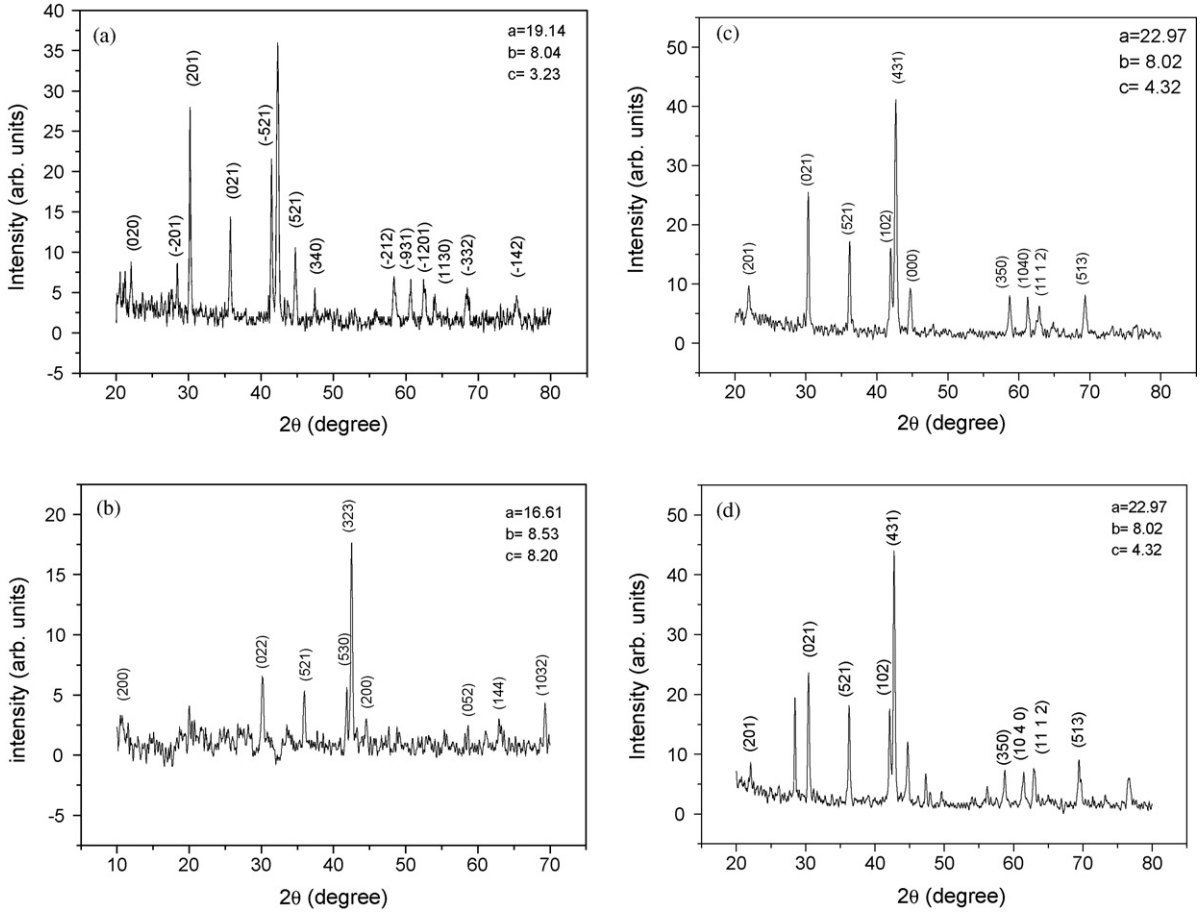

Fig. 1. (a) X-ray diffractogram of sample with La/Ce ratio about 0.5. (b) X-ray diffractogram of sample with La/Ce ratio about 1.0. (c) X-ray Diffractogram of sample with La/Ce ratio about 10.00. (d). X-ray Diffractogram of sample with La/Ce ratio about 15.00.

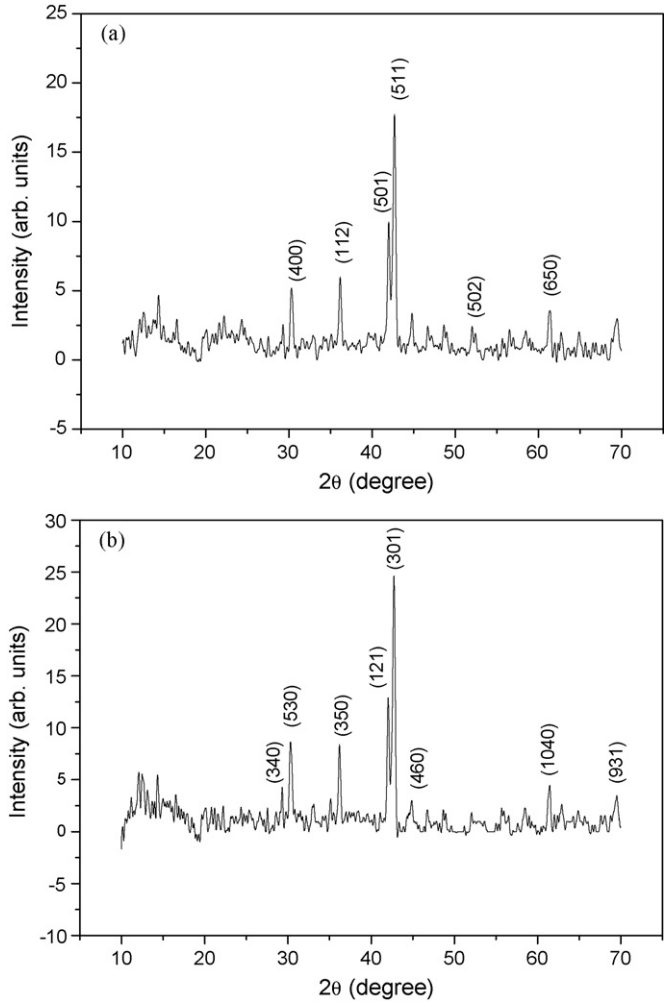

Fig. 2. (a) X-ray Diffractogram of high Mn content sample with La/Ce ratio about 0.5. (b) X-ray Diffractogram of high Mn content sample with La/Ce ratio about 12.

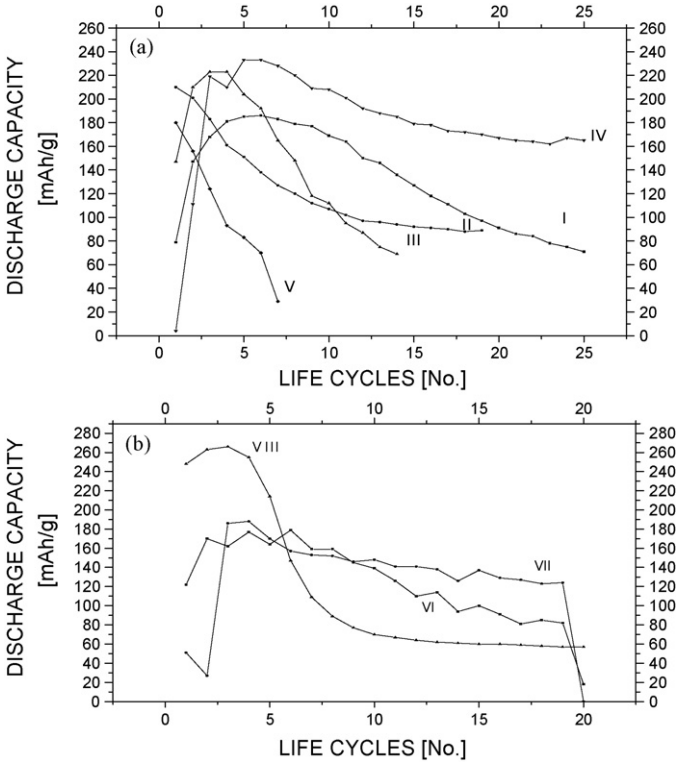

Fig. 3. (a) Life cycling of MH alloys with low Mn content. (b) Life cycling of MH alloys with high Mn content.

influenced mainly by two factors: surface passivation due to oxidation of active composition and pulverization of alloy particles resulting from repeated volume changes during the hydrogen absorption/desorption processes [19]. Among the two, the latter seems to be more crucial in influencing the cycling stability of alloy electrodes since the alloys contain the same constituent elements [26]. The anti-pulverization capability depends on the strength and toughness of the alloy. Generally, grain refinement and formation of an amorphous phase increase the strength and toughness of the alloy. This could enhance the cycle life of the alloy significantly. In addition, the amorphous phase can enhance the anti-corrosion ability of the alloy in corrosive electrolytes, further enhancing the cycle life of the alloy.

It can be inferred from our results that La/Ce ratio has a definite influence on the discharge performance of the alloy, especially on the maximum discharge capacity. As described in a previous work [27], the activation time and the cycle life of the electrodes depend on the effect of hydrogen absorption and on the structure of the alloy crystalline unit cell. Also, substituting Mm with La leads to an obvious change in the microstructure of the alloys. The capacity output varies from 179 to 266 mAh g^{-1}.

A detailed analysis of the results in terms of the composition of the alloys can be seen in the following sections.

The influence of the La/Ce ratio on the performance of the samples is shown in Table 2. It can be seen that in most of the samples, the maximum discharge capacity increases with La/Ce ratio up to a value of about 12 and decreases thereafter. This is true with samples with low and high Mn contents. This implies that the amount of rare earth in the alloy has a significant effect on the performance. Furthermore, the amount of rare earth is an essential factor that determines the maximum capacity output. In fact, samples with the maximum capacity had a high La/Ce ratio, around 12. This is due to the fact that substituting Mm with La influences crystal orientation during the alloy crystallization process [17]. The lattice constants and cell volumes of the alloys increase with increase in the amount of Mm. It is generally accepted that hydrogen storage alloys with larger unit cell volumes would result in more sites available for hydrogen storage. An increase in cell volume as well as grain refinement is favorable for the diffusion of hydrogen atoms. The smaller the grain size and larger the crystal boundary area, the more are the channels for hydrogen diffusion. Factors such as those above that facilitate the diffusion capability of hydrogen improve the activation capability and discharge rate capability of the alloys.

An analysis of the life cycle profiles of different categories of samples with different rare earth contents reveals interesting results. The samples I, II, VI and VII have La/Ce ratios less than 1. Sample I attains a stable, but low capacity for an extended number of cycles after a regular decline from a high capacity. Sample II, after an initial increase, shows a parabolic

Table 3
Influence of rare earth content (La/Ce) on activation performance

ALLOY	(La/Ce) Ratio	*n*
Samples with low Mn content		
I	0.51	6
II	0.99	1
III	9.49	3
IV	12.55	6
V	18.73	1
Samples with high Mn content		
VI	0.52	4
VII	0.64	4
VII	11.65	3

fall in capacity. Sample VI, after an initial increase and stability, exhibits a regular fall followed by steep fall in the concluding stages. Sample VII shows a regular decline with an onset of a sudden drop after 20 cycles. In general, most of the samples either show a regular fall or a fall after an initial increase.

Samples IV and VII have very high La/Ce ratios, i.e. above 10. Sample VII after an initial increase shows a rapid fall in capacity up to 8 cycles, a fairly stable capacity for a further 15 cycles, followed by a rapid decrease. Sample IV, after requiring few cycles for activation, shows a rapid fall in capacity up to 20 cycles and thereafter shows a fairly stable capacity in the next 80 cycles. Thus, it is seen that despite belonging to the same class of materials with very high La/Ce ratios, there are wide variations in the discharge patterns. It seems difficult to generalize their behavioral pattern.

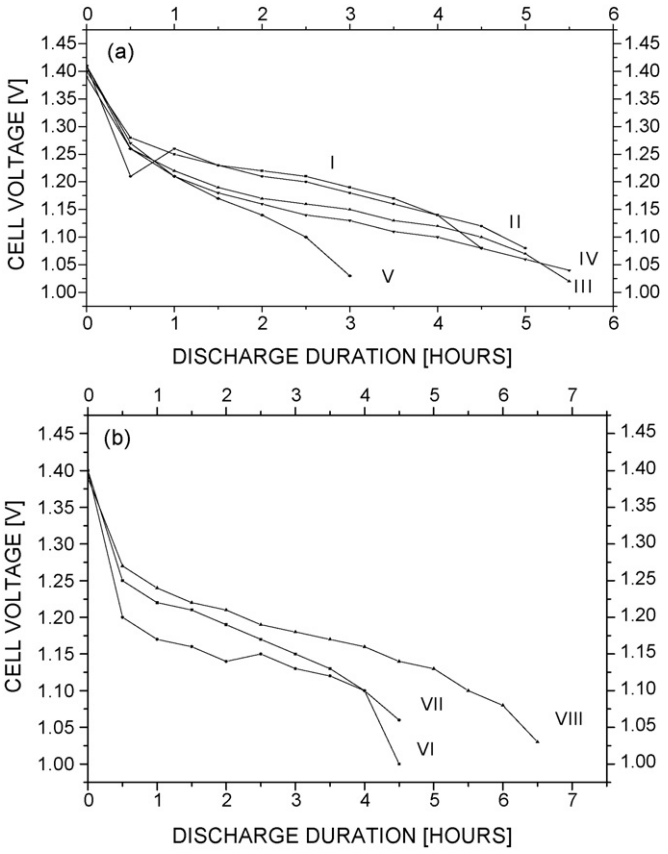

Fig. 4. (a) Discharge patterns of MH alloys with low Mn content. (b) Discharge patterns of MH alloys with high Mn content.

3.2.2. Activation performance

The activation performance is characterized by the initial activation number. The initial activation number, *n*, is defined as the number of charge–discharge cycles required to attain the maximum discharge capacity through a charge–discharge cycle at a constant current drain. Generally, the activation performance of the alloy is closely related to its phase structure, surface characteristics, grain size and interstitial dimensions. It is also directly relevant to changes in the internal energy of the system before and after hydrogen absorption. The larger the additive internal energy (which originates from the oxidation film formed on the surface of the electrode alloy) and greater the strain energy (which is produced by hydrogen atoms entering the interstitials of the tetrahedral or octahedral of the alloy lattice), the poorer is the activation performance of the alloy [28]. Moreover, the initial activation capability could decrease due to an increase in lattice stress and the formation of an amorphous phase [29].

The activation numbers of the alloys are shown in Table 3. Even though no regular trend could be seen from the results, it appears that an increase in the La/Ce ratio facilitates easy activation. This could be attributed to a refinement in grain size and to interstitial dimensions resulting from La enhancement.

3.2.3. Discharge pattern curves

Discharge profiles of the samples are shown in Fig. 4(a and b). It can be seen that except in some cases the shape of the

Table 4
Detailed analysis of discharge patterns

Alloy	(La/Ce) Ratio	First Range	Second Range	Comments
Samples with low Mn content				
I	0.51	1.40–1.27	1.27–1.14	Sloping II Portion
II	0.99	1.42–1.20	1.25–1.07	A kink before onset of II curve
III	9.49	1.38–1.25	1.25–1.02	Oscillations in II Portion
IV	12.55	1.42–1.275	1.275–1.04	Sloping II Portion
V	18.73	1.41–1.26	1.26–1.10	Sloping II Portion
Samples with high Mn content				
VI	0.52	1.40–1.25	1.25–1.10	Flat II Portion
VII	0.64	1.40–1.20	1.20–1.10	Oscillations in II Portion
VII	11.65	1.38–1.27	1.27–1.07	Sloping II Portion

discharge curves are nearly same for all the alloys. A detailed analysis of the discharge profiles is given in Table 4.

4. Conclusions

Our results reveal that the discharge capacity of samples with La/Ce ratios 0.51–18.73 varies between 179 and 266 mAh g^{-1}. As per expectations, the rare earth content has a significant effect on the performance of the alloy. It is concluded that the amount of rare earth in the alloys is an essential requirement in order to realize high capacities. The optimum La/Ce ratio is 12. Moreover, the definitive influence of the La/Ce ratio on the alloy performance can be traced to its crystal structure.

Acknowledgements

The authors thank the Director, CECRI, Karaikudi for encouragement and permission to publish this work. Thanks are due to MNES, New Delhi for sanctioning a Grant-In-Aid project on 'Development of advanced Ni-MH battery-fitted electric bicycle and field studies' under which the above work was carried out. The authors also thank Dr. N.G. Renganathan for providing necessary facilities and Dr. M. Ganesan for recording XRF data. One of the authors, LMN, thanks the Director, CECRI for permission to carry out her MSc project work.

References

[1] C.J. Winter, Int. J. Hydrogen Energy 29 (2004) 1095.
[2] G. Sandrock, R.C. Bowman Jr., J. Alloys Compd. 356–357 (2003) 794.
[3] F. Cuevas, J.M. Joubert, M. Latroche, A. Percheron-Guégan, Appl. Phys. A72 (2001) 225.
[4] M. Golben, D.H. DaCosta, Proceeings of 2001 DOE Hydrogen Program Review NREL/CP-570-30535, 2001.
[5] Z. Dehouche, N. Grimard, F. Laurencelle, J. Goyette, T.K. Bose, J. Alloys Compd. 399 (2005) 224.
[6] E. Willers, M. Wanner, M. Groll, J. Alloys Compd. 293–295 (1999) 915.
[7] J.G. Park, K.J. Jang, P.S. Lee, J.Y. Lee, Int. J. Hydrogen Energy 26 (2001) 701.
[8] R.C. Bowman Jr., J. Alloys Compd. 356–357 (2003) 789.
[9] Y. Tang, H. Chen, J. Jiang, Z. Tang, B. Huang, H.W. Roesky, J. Power Sources 130 (2004) 56.
[10] T. Sakai, M. Matsuoka, C. Iwakura, in: L. Eyring (Ed.), Handbook of the Physics and Chemistry of Rare Earths, Elesvier, Amsterdam, 1995, p. 133.
[11] F. Feng, M. Geng, D.O. Northwood, Int. J. Hydrogen Energy 26 (2001) 725.
[12] I. Uehara, T. Sakai, H. Ishikawa, J. Alloys Compd. 253/254 (1997) 635.
[13] Q.D. Wang, C.P. Chen, Y.Q. Lei, J. Alloys Compd. 253–254 (1997) 629.
[14] X. He, J. Li, H. Cheng, C. Jiang, C. Wan, J. Power Sources 152 (2005) 285.
[15] B. Rozdzynska-Kielbik, W. Iwasieczko, H. Drulis, V.V. Pavlyuk, H. Bala, J. Alloys Compd. 298 (2000) 237.
[16] G. Smith, A.J. Goudy, J. Alloys Compd. 316 (2001) 93.
[17] Y. Zhang, G.Q. Wang, X.P. Dong, S.H. Guo, J.Y. Ren, X.L. Wang, J. Power Sources 148 (2005) 105.
[18] G. Sandrock, J. Alloys Compd. 293–295 (1999) 877.
[19] J.J. Reilly, in: J.O. Besenhard (Ed.), Handbook of Battery Materials, Wiley, New York, 2000.
[20] B. Liao, Y.Q. Lei, L.X. Chen, G.L. Lu, H.G. Pan, Q.D. Wang, J. Power Sources 129 (2004) 358.
[21] W.K. Hu, J. Alloys Compd. 297 (2000) 206.
[22] Y.H. Zhang, X.P. Dong, G.Q. Wang, S.H. Guo, X.L. Wang, J. Power Sources 140 (2005) 381.
[23] A. Ticianelli, S. Mukerjee, J. McBreen, G.D. Adzic, J.R. Johnson, J.J. Reilly, J. Electrochem. Soc. 146 (1999) 3582.
[24] G.D. Adzic, J.R. Johnson, J.J. Reilly, J. McBreen, S. Mukerjee, M.P.S. Kumar, W. Zhang, S. Srinivasan, J. Electrochem. Soc. 142 (1995) 3429.
[25] M.P.S. Kumar, W. Zhang, K. Petrov, A.A. Rostami, S. Srinivasan, G.D. Adzic, J.R. Johnson, J.J. Reilly, H.S. Lim, J. Electrochem. Soc. 142 (1995) 3424.
[26] F.L. Zhang, Y.C. Luo, J.P. Chen, R.X. Yan, L. Kang, J.H. Chen, J. Power Sources 150 (2005) 247.
[27] T. Vogt, J.J. Reilly, J.R. Johnson, G.D. Adzic, J. McBreen, J. Electrochem. Soc. 146 (1999) 15.
[28] Y. Zhou, Y. Lei, Y. Luo, S. Cheng, Q. Wang, Acta Metall. Sinica 32 (1996) 857.
[29] Y.H. Zhang, G.Q. Wang, X.P. Dong, S.H. Guo, X.L. Wang, J. Power Sources 137 (2004) 309.